Session 2.3
Non-invasive approaches – new imaging and remote techniques (Doerenkamp-Zbinden Session)

Magnetic Resonance Imaging of Animal Brain *In Vivo*

Jens Frahm, Susann Boretius, Takashi Watanabe and Thomas Michaelis
Biomedizinische NMR Forschungs GmbH, Max-Planck-Institut für biophysikalische Chemie, D-Göttingen, Germany

Summary
As a non-invasive tool for mapping anatomical and functional aspects of the central nervous system, magnetic resonance imaging (MRI) reduces the number of animals in follow-up examinations and refines the quality of the results by yielding in vivo data of individual animals over extended time periods. Although applications cover the full range from non-human primates to insects, the vast majority of MRI studies focuses on rodents. This work illustrates selected applications in mice based on three-dimensional images at almost 100 mm isotropic spatial resolution. A primary aim is a better understanding of the pathophysiological mechanisms underlying human brain disorders. In this respect, the cuprizone mouse model allows the identification of MRI markers for demyelination and remyelination. Complementary, the use of transgenic mice with a Cnp1 deficiency in oligodendrocytes adds selective MRI studies of axonal damage without demyelination. A second goal is the functional assessment of synaptic activity and axonal transport in various brain systems using manganese-enhanced MRI. The contrast agent identifies activity-dependent regional differences in the mouse hippocampus and delineates the efferent pathways to the ventral hippocampal commissure and septal region. While opening the way for investigations of memory and learning in mutant mice, corresponding studies of the habenulo-interpeduncular system provide links to cognition and behaviour and the mechanisms of neuropsychiatric diseases.

Keywords: axonal damage, axonal transport, cuprizone, demyelination, magnetic resonance imaging, manganese, mouse, remyelination

Introduction

Over the past two decades, magnetic resonance imaging (MRI) has gained tremendous importance – not only in the clinic but also in animal research. This particularly applies to the field of neuroscience and studies of the intact living brain, for example see (Natt and Frahm, 2004). Instead of using a human whole body MRI system, most animal studies are better served with a dedicated small-bore magnet and a suitable array of radio frequency antennae for MRI signal excitation and detection.

Apart from being non-invasive, MRI not only offers access to anatomical structures at high spatial resolution using true three-dimensional (3D) image acquisition, but also yields excellent soft-tissue contrast and marked sensitivity to pathological tissue alterations. Specificity is slightly less pronounced, but at least in part compensated for, by a variety of different MRI techniques, which complement morphological assessments by giving insight into brain metabolism and function. While applications in animal research range from monkeys to insects, for example see (Boretius et al., 2004 and Michaelis et al., 2005), studies of non-human primates or their immediate precursors are rare and only prompted by the need for immunological or behavioural properties that are similar to those of humans. The vast majority of animal MRI studies focuses on rodents.

In general, MRI turns out to be particularly attractive for animal experimentation. First of all, the approach reduces the number of animals required in follow-up studies of disease progression or therapy. Secondly, MRI refines the quality of the data by yielding *in vivo* rather than *post mortem* parameters and by allowing the monitoring of *individual* animals without necessarily relying on group comparisons. Thirdly, studies of mutant animals offer the chance to link molecular biology and neurogenetics to physiological and functional properties at the system

level. And finally, clinical MRI studies may be complemented by new approaches not yet or not directly applicable to humans. The purpose of this work is to illustrate these concepts by a couple of selected applications in mice.

Animals

All studies were performed in accordance with the European Council Directive (86/609/EEC) and approved by the responsible governmental authority (*Bezirksregierung Braunschweig*). Animals were individually housed under conventional conditions in macrolon cages according to the recommendations of the Society for Laboratory Animal Science (Germany).

Magnetic resonance imaging

Mice were anaesthetised by i.p. injection of medetomidine (1.5 mg/kg) and ketamine (150 mg/kg) for induction. Subsequently, animals were intubated with a polyethylene endotracheal tube and artificially ventilated. Anaesthesia was maintained using 0.5-1.0% isoflurane in oxygen and respiration was monitored by a signal derived from a homemade pressure transducer fixed to the animal's chest. For MRI the animals were placed in a prone position on a purpose-built holder with an adjustable nose cone. The rectal temperature was held constant at 37 ± 1° by covering the body with water blankets. Figure 1 shows the experimental set-up for MRI studies of mouse brain. During the examination, the holder is positioned in the centre of a horizontal magnet. The use of inhalation anaesthesia allows examination for up to 3 hours as well as repeated follow-up studies of individual animals.

All MRI studies were conducted at 2.35 T using an MRBR 4.7/400-mm magnet (Magnex, Scientific, Abington, UK) equipped with a DBX system (Bruker Biospin, Ettlingen, Germany). Radio frequency excitation was accomplished by use of a whole-body Helmholtz coil (100 mm) and combined with an elliptical surface coil (20 x 12 mm) for MRI signal detection. Three-dimensional T1-weighted (3D FLASH, repetition time TR = 17 ms, echo time TE = 7.58 ms, flip angle 25°) and T2-weighted images (3D FSE, TR/TE = 3000/98.25 ms, 16 echoes, echo-spacing = 12.5 ms) were obtained with an isotropic spatial resolution of 117 μm (Natt et al., 2002). Maps of the magnetisation transfer ratio (MTR) were based on a spin density-weighted sequence (3D FLASH, TR/TE = 30/7.60 ms, flip angle 5°) with and without off-resonance radio frequency irradiation (frequency offset: 5 kHz, mean amplitude: 200 Hz corresponding to a flip angle of 1045°) (Natt et al., 2003).

Results and discussion

High-resolution 3D MRI of mouse brain *in vivo*

High-quality three-dimensional images of the brain of anaesthetised mice may be obtained at almost 100 mm isotropic spatial resolution within measuring times of 1-2 hours. Figure 2 shows selected sections from T1-weighted 3D MRI acquisitions of two different mouse strains depicting pronounced differences in ventricular volume (Natt et al., 2002). MRI provides reliable access to small structures including the hippocampal formation or the habenular nuclei – truly in three dimensions and with the possibility of arbitrary image reconstructions. Complementary

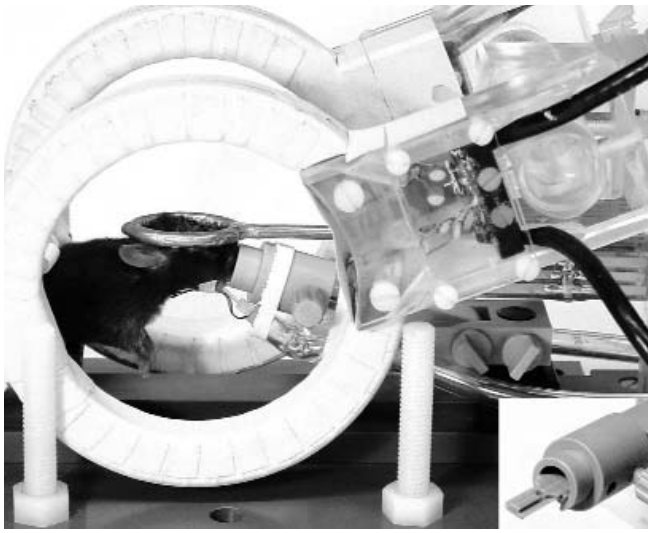

Fig. 1: Experimental set-up for MRI of mouse brain *in vivo*.
Animals are intubated for inhalation anaesthesia and warmed by water-filled blankets. MRI signal excitation and detection is accomplished by use of a large Helmholtz coil (100 mm diameter) surrounding the whole animal and a small elliptical surface coil (20 mm anterior-posterior, 12 mm left-right) atop the head, respectively. The insert (right bottom corner) depicts the head holder comprising a nose cone and bite bar.

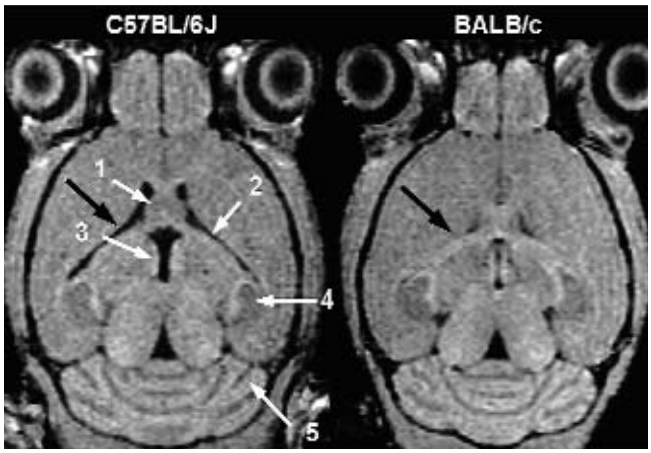

Fig. 2: High-resolution T1-weighted MRI of mouse brain *in vivo*.
The images represent selected sections of a 3D MRI acquisition at 117 mm isotropic resolution (for details see text) in two different strains. C57BL/6J and BALB/c mice present with structural variations such as relatively large ventricles in the forebrain of C57BL/6J animals (black arrows). 1 = Lateral septum, 2 = hippocampal fimbria, 3 = medial habenular nucleus, 4 = hippocampal formation, 5 = cerebellar folia. Adapted from (Natt et al., 2002).

to images with T1 contrast as shown here, many applications rely upon additional T2-weighted images because of their particular sensitivity to detect pathological tissue alterations (see below).

Cuprizone mouse model: MRI of changes in myelination

Mouse models are extensively used to study the pathophysiological mechanisms of multiple sclerosis (MS). This is largely because human MRI studies of MS lesions are hampered by the occurrence of pronounced heterogeneity and the simultaneous presence of inflammation, demyelination (and remyelination), and axonal damage as the pathologic hallmarks of this autoimmune disorder.

Complementary to the widespread use of animal models of experimental allergic encephalitis (EAE), the cuprizone mouse model specifically addresses the aspects of demyelination and remyelination. Feeding mice with cuprizone leads to a selective and reversible demyelination of the corpus callosum with little or no axonal damage (Johnson and Ludwin, 1981; Matsushima and Morell, 2001). The effect has been demonstrated by histological staining for myelin and is also well characterised by MRI as shown in figure 3 (Merkler et al., 2005). In comparison to controls with normal myelination, as for example visualised by a dark corpus callosum on T2-weighted images, demyelination after 6 weeks of cuprizone causes a reversal of contrast that is a bright intensity on T2-weighted images. After another 6 weeks of normal diet, the animals exhibit partial remyelination of white matter and a respective partial recovery of MRI contrasts. It could be shown that a combination of all three MRI contrasts depicted in figure 3, namely T2, T1, and magnetisation transfer contrast, correctly differentiated 95% of all animals as myelinated, demyelinated, or remyelinated when using a discriminant function analysis (Merkler et al., 2005).

The ability to non-invasively predict the myelin status promises new insights into the evolution of MS lesions. It certainly represents a prerequisite for the *in vivo* monitoring and evaluation of novel therapeutic approaches devised to promote re-myelination. Pertinent strategies include the application of growth factors, the transplantation of myelin-forming stem cells or the use of intravenous immunoglobulin therapies.

Cnp1 deficient mice: MRI of axonal damage

In analogy to the cuprizone mouse model of demyelination, the use of transgenic mice with a Cnp1 deficiency in oligodendrocytes (Lappe-Siefke et al., 2003) offers selective MRI studies of axonal damage as another pathophysiological mechanism in MS and other neurodegenerative disorders. The gene encodes a protein which turns out to be essential for axonal survival but not for myelin assembly. Accordingly, Cnp1 deficient mice develop

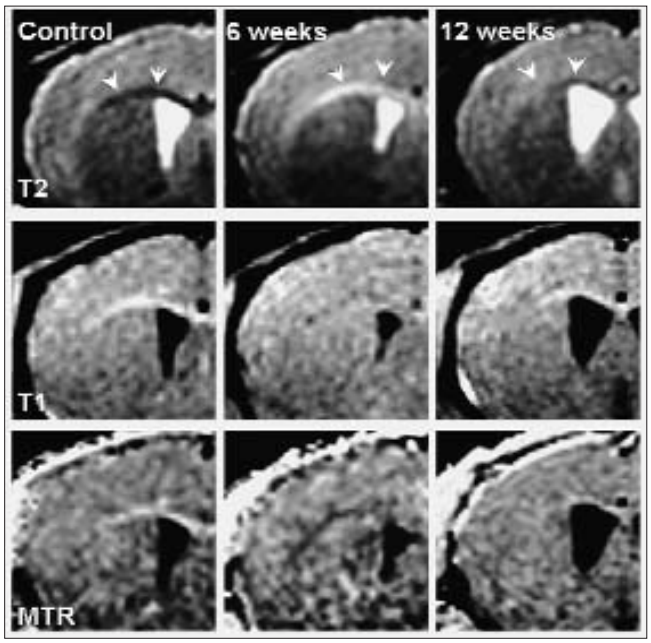

Fig. 3: MRI of myelination in mice treated with cuprizone. In comparison with controls, animals show pronounced demyelination of the corpus callosum (arrowheads) after 6 weeks of cuprizone treatment. The effect is best seen by a reversal of T2 contrast, that shows hypointensities for controls and hyperintensities at 6 weeks, as well as by a reduction of both T1 contrast and the magnetisation transfer ratio (MTR). After an additional 6 weeks on normal diet and withdrawal of the toxin (12 weeks), T1 and T2 contrast as well as MTR partially recover indicating remyelination. Adapted from (Merkler et al., 2005).

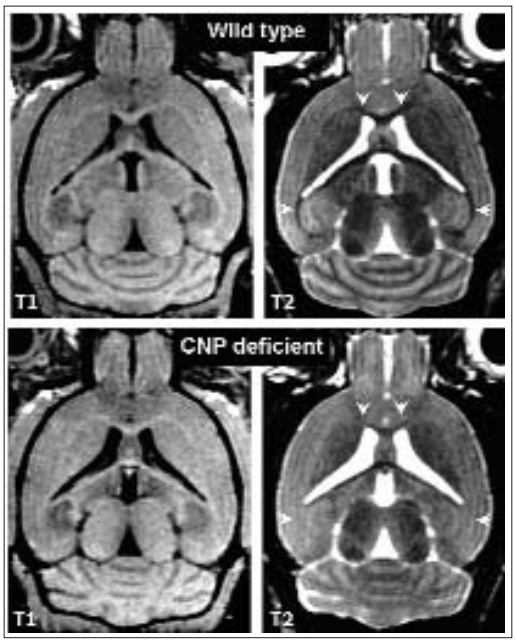

Fig. 4: MRI of axonal damage in *Cnp1*-deficient mice. Mice with a deficiency of the *Cnp1* gene in oligodendrocytes develop axonal damage while maintaining myelin structure and function. *Cnp1* deficient mice at the age of 12 months reveal a reduction or even a complete lack of T2 contrast in the corpus callosum and hippocampal fimbria (arrowheads) without alterations of T1 contrast. This pattern differs from the MRI findings for demyelination (see Figure 3).

axonal swelling and neurodegeneration throughout the brain without demyelination.

MRI of *Cnp1* deficient mice reveals no changes in T1-weighted images of white matter structures but a lack of contrast in T2-weighted images. These observations represent a pattern that clearly differs from the MRI findings for demyelination (see previous section). As demonstrated in figure 4, the exclusive T2 changes not only apply to the corpus callosum but also to the hippocampal fimbria. Moreover, the mutants exhibit altered diffusion properties and reduced brain volumes. Together, these preliminary findings may lead to new in vivo markers of axonal damage.

Functional staining of neuroaxonal connectivity using Mn^{2+}-enhanced MRI

Extending structural characterisations, contrast-enhanced MRI aims at functional assessment of synaptic activity and activity-dependent axonal transport in various brain systems. The concept is based on the application of divalent manganese ions (Mn^{2+}) that, similar to calcium ions (Ca^{2+}), are taken up by voltage-gated calcium channels into active neurons. At the same time, Mn^{2+} ions serve as MRI contrast agent, shortening the T1 relaxation time (Lin and Koretsky, 1997; Pautler et al., 1998). Thus, Mn^{2+}-enhanced images with hyperintensities in areas of specific uptake or accumulation may be recorded at high spatial resolution using T1-weighted 3D MRI. As an early example, the intravitreal application of $MnCl_2$ into one eye of a rat delineated the entire visual pathway from the optic nerve, chiasma, contralateral optic tract, and lateral geniculate to the superior colliculus and suprachiasmatic nucleus (Watanabe et al., 2001).

Subsequently, Mn^{2+}-enhanced 'staining' of specific brain systems and their axonal connections has been exploited for functional mapping of hippocampal projections after bilateral intraparenchymal injection (Watanabe et al., 2004a). Figure 5 reveals a regionally selective enhancement within the hippocampal formation thath almost exclusively affects the dentate gyrus and CA3 subfield with only very mild extensions into CA1 and the subiculum. This pattern is in line with differences in the excitability of hippocampal neurons previously seen in electrophysiologic recordings. Uptake is mainly in active pyramidal cells, which is further supported by the axonal projections toward the lateral septum shown in figure 6. Taken from the same 3D MRI data set as the image shown in figure 5, sections anterior to the hippocampus delineate the efferent hippocampal pathways to the ventral hippocampal commissure and the septal region by enhancement in the fimbria, ventral hippocampal commissure, precommisural fornix, and septal nuclei (Watanabe et al., 2004a). In conjunction with suitable cognitive tasks and behavioural assessments, high-resolution Mn^{2+}-enhanced MRI of normal and mutant mice is expected to become a powerful tool for a further characterisation of learning and memory processing in the hippocampal system.

The functional relevance of manganese contrast is further evidenced by observations after injection into the lateral ventricle or after systemic subcutaneous administration, in which case Mn^{2+}-uptake into the central nervous system is accomplished via the CSF-brain barrier (Watanabe et al., 2002). Figure 7 shows the uptake of manganese into active neurons of the habenulo-interpeduncular system where the initial enhancement of the habenula is followed by MRI signal increases of the fasciculus retroflexus as the connecting axonal tract and finally the interpeduncular nucleus (Watanabe et al., 2004b). Though not directly visible in a single 3D MRI scan, the sequential enhancement may be demonstrated by repetitive 3D MRI recordings.

While the hippocampal formation is involved in learning and memory, the habenular complex is a crucial relay structure in the diencephalic conduction system and is as such involved in cog-

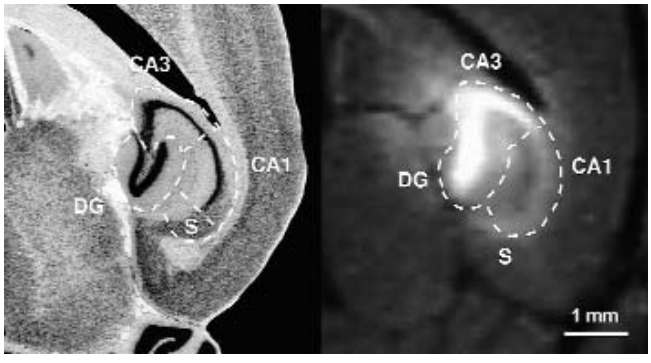

Fig. 5: Manganese-enhanced MRI of the mouse hippocampus.
The mouse hippocampal formation in (left) a histologic section (Cresyl violet, adapted from Rosen et al., 2000) and (right) a corresponding T1-weighted section from a 3D MRI data set 6 hours after intraparenchymal injection of $MnCl_2$ (0.25 µl, 200 mM). Pronounced signal enhancements in the dentate gyrus (DG) and CA3 subfield are complemented by only very mild signal increases in the CA1 subfield and subiculum (S). Adapted from (Watanabe et al., 2004a).

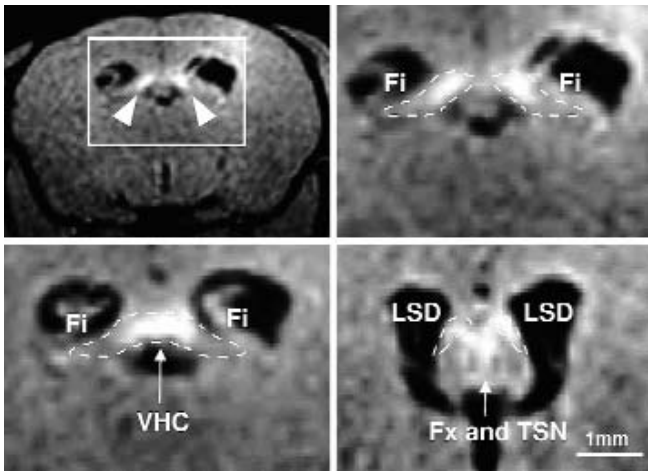

Fig. 6: Manganese-enhanced MRI of the mouse hippocampal projections.
Selected sections (magnified views) along the hippocampo-septal projection pathway 6 hours after intraparenchymal injection of $MnCl_2$ (same T1-weighted MRI data set as shown in Figure 5) depict enhanced structures such as the medial part of the fimbria (Fi) bilaterally, the ventral hippocampal commissure (VHC), the dorsal part of the lateral septal nucleus (LSD) bilaterally, the precommissural fornix (Fx), and the triangular septal nucleus (TSN). Adapted from (Watanabe et al., 2004a).

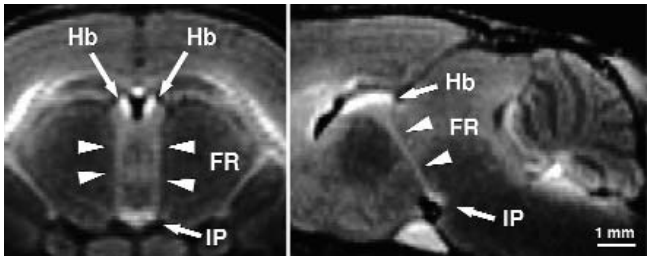

Fig. 7: Manganese-enhanced MRI of the mouse habenulo-interpeduncular system.
The images represent (left) an oblique section and (right) a parasagittal section of a 3D MRI data set 6 hours after intraventricular injection of $MnCl_2$ (0.25 ml, 5 mM). They demonstrate enhancement in the anterior parts of the habenulae (Hb), the fasciculus retroflexus (FR) as its major axonal connection, and the interpeduncular nucleus (IP). Adapted from (Watanabe et al., 2004b).

nition and behaviour, for example as part of the reward system. As an example, functional Mn^{2+}-enhanced MRI may therefore offer completely new ways to study mutant mice with – or without – recently discovered susceptibility genes for neuropsychiatric diseases such as schizophrenia.

Conclusion

The most prominent advantage of MRI is the fact that the procedure itself is non-invasive. MRI helps to reduce the number of animals used and improves the quality of the research by yielding *in vivo* rather than *post mortem* results, as well as by monitoring disease progression or therapeutic efficacy in *individual* animals. Multiple techniques offer insights into the anatomy, metabolism, and function of the central nervous system for a wide range of species. Thus, MRI contributes to bridging basic and clinical neuroscience and emerges as a key tool in translational research.

References

Boretius, S., Natt, T., Watanabe, T., Ehrenreich, L., Tammer, R., Frahm, J. and Michaelis, T. (2004). In vivo diffusion tensor mapping of the brain of squirrel monkey, rat, and mouse using single-shot STEAM MRI. *MAGMA 3*, 1-9.

Johnson, E.S. and Ludwin, S.K. (1981) The demonstration of recurrent demyelination and remyelination of axons in the central nervous system. *Acta Neuropathol. 53*, 93-98.

Lappe-Siefke, C., Goebbels, S., Gravel, M., Nicksch, E., Lee, J., Braun, P.E., Griffiths, I.R. and Nave, K.A. (2003) Disruption of Cnp1 uncouples oligodendroglial functions in axonal support and myelination. *Nat. Gen. 33*, 366-374.

Lin, Y.J. and Koretsky, A.P. (1997) Manganese ion enhances T_1-weighted MRI during brain activation: an approach to direct imaging of brain function. *Magn. Reson. Med. 38*, 378-388.

Matsushima, G.K. and Morell, P. (2001) The neurotoxicant, cuprizone, as a model to study demyelination and remyelination in the central nervous system. *Brain. Pathol. 11*, 107-116.

Merkler, D., Boretius, S., Stadelmann, C., Ernsting, T., Michaelis, T., Frahm, J. and Brück, W. (2005). Multicontrast MRI of remyelination in the central nervous system. *NMR Biomed. 18*, in press.

Michaelis, T., Watanabe, T., Natt, O., Boretius, S., Frahm, J., Utz, S. and Schachtner, J. (2005). In vivo 3D MRI of insect brain: Cerebral development during metamorphosis of Manduca Sexta. *NeuroImage 24*, 596-602.

Natt, O., Watanabe, T., Boretius, S., Radulovic, J., Frahm, J. and Michaelis, T. (2002). High-resolution 3D MRI of mouse brain reveals small cerebral structures in vivo. *J. Neurosci. Meth. 120*, 203-209.

Natt, O., Watanabe, T., Boretius, S., Frahm, J. and Michaelis, T. (2003). Magnetization transfer MRI of mouse brain reveals areas of high neural density. *Magn. Reson. Imaging 21*, 1113-1120.

Natt, O. and Frahm, J. (2004). In vivo magnetic resonance imaging: Insights into structure and function of the central nervous system. *Meas. Sci. Technol. 16*, R17-R36.

Pautler, R.G., Silva, A.C. and Koretsky, A.P. (1998) In vivo neuronal tract tracing using manganese-enhanced magnetic resonance imaging. *Magn. Reson. Med. 40*, 740-748.

Rosen, G.D., Williams, A.G., Capra, J.A., Connoly, M.T., Cruz, B., Lu, L., Airey, D.C., Kulkarni, K. and Williams, R.W. (2000). The mouse brain library@www.mbl.org Int. Mouse *Genome Conf. 14*, 166.

Watanabe, T., Michaelis, T. and Frahm, J. (2001). Mapping of retinal projections in the living rat using high-resolution 3D gradient-echo MRI with Mn^{2+}-induced contrast. *Magn. Reson. Med. 46*, 424-429.

Watanabe, T., Natt, O., Boretius, S., Frahm, J. and Michaelis, T. (2002). In vivo 3D MRI staining of mouse brain after subcutaneous application of $MnCl_2$. *Magn. Reson. Med. 48*, 852-859.

Watanabe, T., Radulovic, J., Spiess, J., Natt, O., Boretius, S., Frahm, J. and Michaelis, T. (2004a). In vivo 3D MRI staining of the mouse hippocampal system using intracerebral injection of $MnCl_2$. *NeuroImage 22*, 860-867.

Watanabe, T., Frahm, J. and Michaelis, T. (2004b). Functional mapping of neural pathways in rodent brain in vivo using manganese-enhanced three-dimensional magnetic resonance imaging. *NMR Biomed. 17*, 554-568.

Correspondence to

Prof. Dr. Jens Frahm
Biomedizinische NMR Forschungs GmbH
Max-Planck-Institut für biophysikalische Chemie
Am Fassberg 11
D-37070 Göttingen, Germany
e-mail: jfrahm@gwdg.de